

A low noise, high fidelity cross phase modulation in multi-level atomic medium

Liangwei Wang(王亮伟), Jia Guan(关佳), Chengjie Zhu(朱成杰), Runbing Li(李润兵), and Jing Shi(石兢)

Citation: Chin. Phys. B, 2021, 30 (**11**): 114204. DOI: 10.1088/1674-1056/ac078d
Journal homepage: http://cpb.iphy.ac.cn; http://iopscience.iop.org/cpb

What follows is a list of articles you may be interested in

Variation of electron density in spectral broadening process in solid thin plates at 400 nm

Si-Yuan Xu(许思源), Yi-Tan Gao(高亦谈), Xiao-Xian Zhu(朱孝先), Kun Zhao(赵昆), Jiang-Feng Zhu(朱江峰), and Zhi-Yi Wei(魏志义)

Chin. Phys. B, 2021, 30 (**10**): 104205. DOI: 10.1088/1674-1056/abf0fe

Phase-shift interferometry measured transmission matrix of turbid medium: Three-step phase-shifting interference better than four-step one

Xi-Cheng Zhang(张熙程), Zuo-Gang Yang(杨佐刚), Long-Jie Fang(方龙杰), Jing-Lei Du(杜惊雷), Zhi-You Zhang(张志友), and Fu-Hua Gao(高福华)

Chin. Phys. B, 2021, 30 (**10**): 104202. DOI: 10.1088/1674-1056/abe92a

Absorption interferometer of two-sided cavity

Miao-Di Guo(郭苗迪) and Hong-Mei Li(李红梅)

Chin. Phys. B, 2021, 30 (**5**): 054202. DOI: 10.1088/1674-1056/abdea4

Dual-function beam splitter of high contrast gratings

Wen-Jing Fang(房文敬), Xin-Ye Fan(范鑫烨), Hui-Juan Niu(牛慧娟), Xia Zhang (张霞), Heng-Ying Xu(许恒迎), and Cheng-Lin Bai(白成林)

Chin. Phys. B, 2021, 30 (**4**): 044205. DOI: 10.1088/1674-1056/abd68d

Controlling the light wavefront through a scattering medium based on direct digital frequency synthesis technology

Yuan Yuan(袁园), Min-Yuan Sun(孙敏远), Yong Bi(毕勇), Wei-Nan Gao(高伟男), Shuo Zhang(张硕), and Wen-Ping Zhang(张文平)

Chin. Phys. B, 2021, 30 (**1**): 014209. DOI: 10.1088/1674-1056/abb665

A low noise, high fidelity cross phase modulation in multi-level atomic medium*

Liangwei Wang(王亮伟)[1], Jia Guan(关佳)[2], Chengjie Zhu(朱成杰)[3,4,†], Runbing Li(李润兵)[5,‡], and Jing Shi(石兢)[1,§]

[1] *Laboratory of Artificial Micro- and Nano-structures of Ministry of Education and School of Physics and Technology, Wuhan University, Wuhan* 430072, *China*

[2] *School of Physics Science and Engineering, Tongji University, Shanghai* 200092, *China*

[3] *School of Physical Science and Technology, Soochow University, Suzhou* 215006, *China*

[4] *Collaborative Innovation Center of Light Manipulations and Applications, Shandong Normal University, Jinan* 250358, *China*

[5] *State Key Laboratory of Magnetic Resonance and Atomic and Molecular Physics, Wuhan Institute of Physics and Mathematics, Chinese Academy of Sciences, Wuhan* 430071, *China*

(Received 1 February 2021; revised manuscript received 23 March 2021; accepted manuscript online 3 June 2021)

We develop a hybrid scheme of cross phase modulation based on electromagnetically induced transparency (EIT) and active Raman gain (ARG) in a multi-level atomic medium. The cross phase modulation, with low loss and without noise, is demonstrated in a room-temperature ^{85}Rb vapor. We show that a π radian nonlinear Kerr phase shift of the signal light relative to a reference light is observed when the signal light is modulated by the phase control field with the low light intensity. We also show that the linear and the third-order absorption can be eliminated via the Raman gain, and the phase noise of the signal light can be ignored when the phase control light is applied in this hybrid scheme.

Keywords: phase modulation, electromagnetically induced transparency, nonlinear Kerr phase shift

PACS: 42.65.Dr, 42.50.Gy **DOI:** 10.1088/1674-1056/ac078d

Quantum computers and quantum information processing technologies are expected to be the critical technique for revolutionizing information science.[1–4] Effective manipulation of photons at single-photon intensity is essential for the next-generation photon communication.[5] So far, based on nonlinear Kerr cross-phase modulation caused by magnetic field and electric field, many schemes used to realize quantum phase gates have been proposed.[6–10] In general, the nonlinear cross-phase modulation in passive media is weak and requires a long propagation distance in solid media.[11] However, in atomic gases, nonlinear effects can be enhanced by choosing different energy levels and transition pathways. Based on these features, strong nonlinear effects can be achieved by using electromagnetic induction transparency (EIT)[12–17] or weakly driven active Raman gain (ARG)[18–28] technologies. In particular, Artoni *et al.* proposed a novel phase-by-phase control mechanism to achieve broadly tunable light phase shifts.[29] Recently, Sun *et al.* proposed a method to realize large polarization-dependent cross modulation between incident weak lights even at the few-photon level.[30] We have also developed a polarization selective Kerr phase-shifting technology,[31,32] in which a weak phase-control field can be used to achieve rapid phase or polarization control and achieve vector gate operation with polarized light in an atomic medium.

For any technologically viable Kerr-effect-based phase gate, three important characteristics must be met. These are lager phase shift, lower loss and no additional phase noise. The π nonlinear Kerr phase shift has been observed in our recent studies using ARG[19] and EIT[33] methods, respectively. However, the other two features are unattainable independently with weakly driven EIT-based methods and ARG-based methods. In EIT methods, the fundamental problem with weakly driven EIT schemes is that the process operates in an absorption mode and the signal wave suffers from significant attenuation and inherently lossy. This influences the efficiency to check the photon numbers and deceases the fidelity of the quantum operations. In ARG methods, the process operates in a stimulated radiation mode and the additional photons participate into the signal wave. This is harmful for the quantum information processing due to the quantum clone effect.

In this paper, we present a hybrid scheme of cross phase modulation based on electromagnetically induced transparency (EIT) and active Raman gain (ARG) in a multi-level atomic medium. The signal wave is propagating in the EIT window and modulated by the phase-control field, in which an ARG process is synchronously applied. The experimental re-

*Project supported by the National Natural Science Foundation of China (Grant Nos. 11774262 and 61975154).

†Corresponding author. E-mail: chengjie.zhu@yahoo.com

‡Corresponding author. E-mail: rbli@wipm.ac.cn

§Corresponding author. E-mail: jshi@whu.edu.cn

© 2021 Chinese Physical Society and IOP Publishing Ltd

sults show that π radian nonlinear Kerr phase shift of signal light relative to a reference light is observed when the signal light is modulated by a phase control field with low light intensity. The linear and the third-order absorption of the signal light can be eliminated by the stimulated Raman process, and the phase noise of the signal light can also be ignored when the phase control light is applied in this hybrid scheme. Our theory matches the experimental results very well.

We consider an ensemble of life-broadened six-level M-type ^{85}Rb atoms system as shown in Fig. 1. The signal field with Rabi frequency $\Omega_{\rm S}$ couples $|1\rangle \leftrightarrow |4\rangle$ transition with one-photon resonance, and also $|3\rangle \leftrightarrow |5\rangle$ transition with one-photon detuning 3.0 GHz. The coupling field with Rabi frequency $\Omega_{\rm C}$ couples $|3\rangle \leftrightarrow |4\rangle$ transition, where the two-photon resonance is satisfied between the signal light and the coupling light. The pumping field with Rabi frequency $\Omega_{\rm P}$ couples $|2\rangle \leftrightarrow |5\rangle$ transition, in which the two-photon resonance is also satisfied between the signal light and the pumping light. To realize a π Kerr phase shift, the phase-control field with Rabi frequency $\Omega_{\rm Ph}$ drives the transition between states $|3\rangle$ and $|6\rangle$.

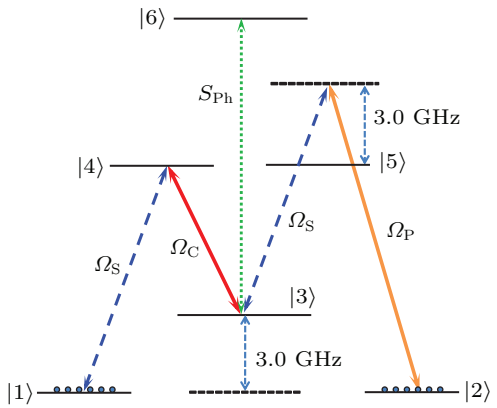


Fig. 1. The scheme of energy levels for cross phase modulation. The signal field couples $|1\rangle \leftrightarrow |4\rangle$ transition with one-photon resonance, and also $|3\rangle \leftrightarrow |5\rangle$ transition with one-photon detuning of 3.0 GHz. The coupling field couples $|3\rangle \leftrightarrow |4\rangle$ transition while the pumping field couples $|2\rangle \leftrightarrow |5\rangle$ transition, where the two-photon resonance is synchronously satisfied. The phase-control field drives $|3\rangle \leftrightarrow |6\rangle$ transition. Here, $\Omega_{\rm P}$, $\Omega_{\rm S}$, $\Omega_{\rm C}$ and $\Omega_{\rm Ph}$ denote the Rabi frequencies of the pump, signal, control and phase control fields, respectively.

Under the rotation wave approximation, the equations of motion for atomic state amplitudes A_j in a six-level atomic system can be written as

$$\left(\mathrm{i}\frac{\partial}{\partial t}+d_2\right)A_2+\Omega_{\rm P}^* A_5=0, \tag{1a}$$

$$\left(\mathrm{i}\frac{\partial}{\partial t}+d_3\right)A_3+\Omega_{\rm C}^* A_4+\Omega_{\rm S}^* A_5+\Omega_{\rm Ph}^* A_6=0, \tag{1b}$$

$$\left(\mathrm{i}\frac{\partial}{\partial t}+d_4\right)A_4+\Omega_{\rm S} A_1+\Omega_{\rm C} A_3=0, \tag{1c}$$

$$\left(\mathrm{i}\frac{\partial}{\partial t}+d_5\right)A_5+\Omega_{\rm S} A_3+\Omega_{\rm P} A_2=0, \tag{1d}$$

$$\left(\mathrm{i}\frac{\partial}{\partial t}+d_6\right)A_6+\Omega_{\rm Ph} A_3=0, \tag{1e}$$

with $\sum_{j=1}^{6}|A_j|^2=1$ and $d_j=\Delta_j+\mathrm{i}\gamma_j$ $(j=2\text{–}6)$. Here, $\Delta_2=2\omega_{\rm S}-\omega_{\rm C}-\omega_{\rm P}-(\omega_2-\omega_1)$, $\Delta_3=\omega_{\rm S}-\omega_{\rm C}-(\omega_3-\omega_1)$, $\Delta_4=\omega_{\rm S}-(\omega_4-\omega_1)$, $\Delta_5=2\omega_{\rm S}-\omega_{\rm C}-(\omega_5-\omega_1)$ and $\Delta_6=\omega_{\rm S}-\omega_{\rm C}+\omega_{\rm Ph}-(\omega_6-\omega_1)$ are detunings with $\hbar\omega_j$ being the energy of state $|j\rangle$; γ_j is the decay rate of the atomic state $|j\rangle$.

Under the slowly varying envelope approximation (SVEA), the Maxwell equation describing the propagation of electromagnetic field $\Omega_{\rm S}$ can be written as

$$\mathrm{i}\left(\frac{\partial}{\partial z}+\frac{1}{c}\frac{\partial}{\partial t}\right)\Omega_{\rm S}+\kappa_{41}A_4A_1^*+\kappa_{53}A_5A_3^*=0, \tag{2}$$

where

$$\kappa_{41}=\mathcal{N}_a|\boldsymbol{\mu}_{14}|^2\omega_{\rm S}/(2\hbar\varepsilon_0 c) \quad \text{and} \quad \kappa_{53}=\mathcal{N}_a|\boldsymbol{\mu}_{35}|^2\omega_{\rm S}/(2\hbar\varepsilon_0 c)$$

with $\mathcal{N}_a$ being the atomic density, ε_0 the vacuum dielectric constant, and c the light speed in vacuum.

Equations (1) and (2) can be solved analytical using the following asymptotic expansion:

$$A_j=\sum_{n=0}^{\infty}\varepsilon^n a_j^{(n)}, \quad (j=1,2,\ldots,6), \tag{3a}$$

$$\Omega_{s,ph}=\sum_{n=1}^{\infty}\varepsilon^n\Omega_{\rm S,Ph}^{(n)}, \tag{3b}$$

where ε is a small parameter characterizing typical amplitude of the signal field Rabi frequency. For the zeroth-order solution (i.e., $n=0$), we can obtain $a_1^{(0)}=a_2^{(0)}=\sqrt{|d_5|^2/(2|d_5|^2+|\Omega_{\rm P}|^2)}$, $a_5^{(0)}=\sqrt{|\Omega_{\rm P}|^2/(2|d_5|^2+|\Omega_{\rm P}|^2)}$, and $a_3^{(0)}=a_4^{(0)}=a_6^{(0)}=0$. In mathematics, to acquire a set of divergence-free solutions in higher-order approximations, all quantities on the right-hand side of the asymptotic expansion must be functions of the multi-scale variables $z_n=\varepsilon^n z$ and $t_n=\varepsilon^n t$ $(n=1\text{–}2)$. Substituting these expansions into Eqs. (1) and (2), we obtain a chain of linear, inhomogeneous equations on $a_j^{(n)}$ and $\Omega_{\rm S,Ph}^{(n)}$, which can be solved order by order.

From Eq. (2), the susceptibility of the signal field follows directly from the equation for the induced polarization, i.e.,

$$P=\mathcal{N}_a(\boldsymbol{\mu}_{14}A_4A_1^*+\boldsymbol{\mu}_{35}A_5A_3^*)=\varepsilon_0\chi_{\rm S}E_{\rm S}, \tag{4}$$

where $\chi_{\rm S}$ represents the susceptibility. In general, $\chi_{\rm S}$ can be Taylor expanded as $\chi_{\rm S}\approx\chi_{\rm S}^{(1)}+\chi_{\rm S}^{(3)}$ with $\chi_{\rm S}^{(1)}$ and $\chi_{\rm S}^{(3)}$ being the linear and nonlinear susceptibilities of the signal field, which read

$$\chi_{\rm S}^{(1)}=\kappa\left[\frac{-(\omega+d_3)|a_1^{(0)}|^2}{(\omega+d_3)(\omega+d_4)-|\Omega_{\rm C}|^2}+\frac{|a_5^{(0)}|^2}{(\omega-d_3^*)}\right], \tag{5a}$$

$$\chi_{\rm S}^{(3)}\approx\kappa\left\{\frac{(\omega+d_3)|a_1^{(0)}|^2}{D_0}\left(\left|\frac{(\omega+d_3)}{D_0}\right|^2+\left|\frac{\Omega_{\rm C}}{D_0}\right|^2\right)|\Omega_{\rm S}^{(1)}|^2+\frac{|a_5^{(0)}|^2}{\omega-d_3^*}\left[\frac{d_2}{(\omega+d_3)D_1}+\frac{d_2^*}{(\omega-d_3^*)D_1^*}\right]|\Omega_{\rm S}^{(1)}|^2\right.$$

$$-\left[\left(\frac{|\Omega_{\rm C}|^2}{D_0^2 d_6}\right)|a_1^{(0)}|^2+\frac{|a_5^{(0)}|^2}{d_6^*(-\omega+d_3^*)^2}\right]|\Omega_{\rm Ph}^{(1)}|^2\Bigg\}, \quad (5b)$$

where $D_0 \equiv (\omega+d_3)(\omega+d_4)-|\Omega_{\rm C}|^2$ and $D_1 \equiv d_2 d_5 - |\Omega_{\rm P}|^2$. Here, the real part of the linear susceptibility [i.e., $\mathrm{Re}(\chi_{\rm S}^{(1)})$] is associated with the phase of the electromagnetic field, while the imaginary part of the susceptibility [i.e., $\mathrm{Im}(\chi_{\rm S}^{(1)})$] is subject to the absorption of the electromagnetic field by the medium. The linear phase and absorption/gain of the signal field are given by $\phi_{\rm L} = k_{\rm S}\mathrm{Re}(\chi_{\rm S}^{(1)})L$ and $\alpha_{\rm L} = k_{\rm S}\mathrm{Im}(\chi_{\rm S}^{(1)})L$, where L is the length of the medium, $k_{\rm S} \equiv \omega_{\rm S}/c$ is the wave vector of the signal field. The Kerr phase shift and the nonlinear (i.e., the third-order) absorption of the signal field can be obtained directly from the nonlinear susceptibility, which are given by $\phi_{\rm NL} = k_{\rm S}\mathrm{Re}(\chi_{\rm S}^{(3)})L$ and $\alpha_{\rm NL} = k_{\rm S}\mathrm{Im}(\chi_{\rm S}^{(3)})L$.

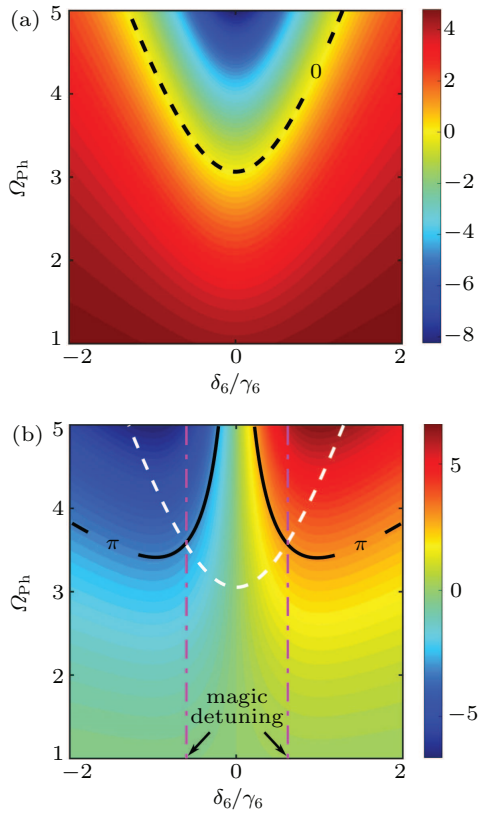


Fig. 2. The total absorption/gain $\alpha_{\rm tot}$ (a) and the phase shift $\phi_{\rm tot}$ (b) as functions of the phase-control field Rabi frequency $\Omega_{\rm Ph}$ and the normalized detuning δ_6/γ_6, respectively. The black dashed curve in (a) denotes $\alpha_{\rm tot}=0$, and the black solid curves in (b) denote $\phi_{\rm tot}=\pm\pi$. The pink dash-dotted lines indicate the magic detunings where a π phase shift can be achieved with zero loss or gain.

For a conventional N-type EIT scheme, the signal field undergoes strong attenuation originated from the linear and nonlinear absorption to obtain large phase shift. With the ARG branch, however, the gain originated from the stimulated Raman process compensates the absorption of the signal field during its propagation. Thus, the absorption or gain of the signal field can be eliminated by adjusting specific intensity and detuning of the signal field. To show this point, we plot the total loss/gain $\alpha_{\rm tot} = \alpha_{\rm L} + \alpha_{\rm NL}$ [Fig. 2(a)] and phase shift $\phi_{\rm tot} = \phi_{\rm L} + \phi_{\rm NL}$ [Fig. 2(b)] of the signal field as functions of the phase control field Rabi frequency $\Omega_{\rm Ph}$ and the detuning δ_6, respectively. Here, the atomic density is chosen as 6×10^{11} cm^{-3}, and other system parameters are given by $\delta_5 = 3$ GHz, $\delta_3 = \delta_4 = 0$ Hz, $\gamma_3 = 200$ kHz, $\gamma_4 = \gamma_5 = \gamma_6 = 300$ MHz, $\Omega_{\rm P} = 20$ MHz, $\Omega_{\rm C} = 15$ MHz and $L = 7.5$ cm. Obviously, the absorption or gain can be eliminated (i.e., $\alpha_{\rm tot}=0$) by choosing a set of specific phase control field Rabi frequency and detuning (see the black dashed curve) as shown in Fig. 2(a). Moreover, there exist two "magic" detunings denoted by the pink dash-dotted lines in Fig. 2(b), where a π phase shift (i.e., $\phi_{\rm tot}=\pm\pi$ indicated by the black solid curves) for the signal field can be achieved without any absorption or gain.

To verify the above theoretical results, the experiments are conducted in a six-level rubidium atom system shown in Fig. 3(a). The length and the diameter of this ^{85}Rb vapor cell are 7.5 cm and 2 cm, respectively. It is filled with 933 Pascal Neon buffer gas and also shielded from ambient magnetic fields under three layers of μ-metal. The temperature of this atomic gas is about 320 K and the atomic density is about 6×10^{11} cm^{-3}. A weak magnetic field with an intensity of 100 mG is applied along the propagation direction of the signal field. Thus, the atomic states of this six-level system is chosen as $|1\rangle \equiv |5S_{1/2},\ F=2,\ m_{\rm F}=-2\rangle$, $|2\rangle \equiv |5S_{1/2},\ F=2,\ m_{\rm F}=0\rangle$, $|3\rangle \equiv |5S_{1/2},\ F=3,\ m_{\rm F}=-1\rangle$, $|4\rangle \equiv |5P_{1/2},\ F=2,\ m_{\rm F}=-2\rangle$, $|5\rangle \equiv |5P_{1/2},\ F=2,\ m_{\rm F}=-1\rangle$, and $|6\rangle \equiv |5P_{3/2},\ F=4,\ m_{\rm F}=-1\rangle$. The linearly polarized signal field and left-circularly polarized coupling (pump) field are collected together by a beam splitter (BS), and propagate along the direction of the magnetic field. Then, the signal field is separated into two lights, where one is the signal field while the other one is utilized as the reference field. After the interaction with the atom, they are combined together by using another beam splitter (BS) to build the optical Mach–Zehnder interferometer. We set a small angle of less than 1° between the pump (coupling) and signal fields so that they are physically separated at a distance of about 1 m from the exit of the vapor cell. To introduce a Kerr phase shift, we inject a weak linear polarized phase-control field with a 3 mm beam diameter and the signal field that are overlapped with opposite propagating directions. In our experiment, the two-photon resonant condition is satisfied between the signal field and the coupling field to obtain the maximum intensity of the signal field.

In the experiment, the coherent fields are generated by an acousto-optic modulator as shown in Fig. 3(b). The coupling field is locked on the transitions between states $|3\rangle$ and $|4\rangle$ of the ^{85}Rb atoms via a saturated absorption spectroscopy, and modulated by the acousto-optic modulator with the offset frequency 3.04 GHz. The signal field is generated by the

+1 order diffracted light of the AOM. The pumping field is generated by the $2\times(+1)$ order diffracted light of the AOM with the double-pass configuration, which is amplified by a tapered amplifier. The strong coupling field with 6 mW intensity and 3 mm beam diameter and the pumping field with 12 mW intensity and 3 mm beam diameter drive $|3\rangle \leftrightarrow |4\rangle$ and $|2\rangle \leftrightarrow |5\rangle$ transitions, respectively. The vertical-polarized signal field with 5 μW intensity and 1 mm beam diameter drives $|1\rangle \leftrightarrow |4\rangle$ and $|3\rangle \leftrightarrow |5\rangle$ transitions simultaneously. Thus the M-type scheme is formed by combining the EIT and ARG schemes. The phase-control field coupling the states $|3\rangle \leftrightarrow |6\rangle$ is applied to observe the cross phase modulation in this hybrid scheme.

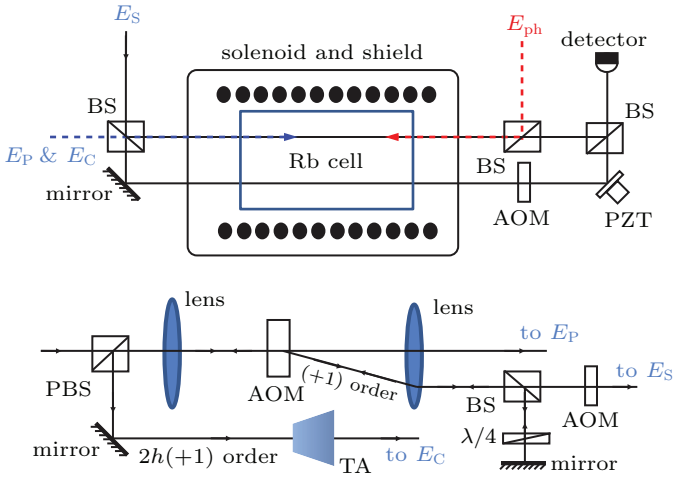


Fig. 3. (a) The experimental setup. (b) The generation of coherent fields. The ^{85}Rb vapor cell is shielded from the ambient magnetic field. An about 100 mG magnetic field is generated by the solenoid, which provides a quantum axis for the atoms. The Mach–Zehnder interferometer is used to observe the nonlinear phase shift.

In the three-level Λ-type EIT, the signal light will transmit the medium when the two-photon resonance conditions are satisfied. In the experiment, the coupling field resonantly drives the transition between states $|3\rangle$ and $|4\rangle$. Carefully adjusting the intensity and one-photon detuning of the pump field, the signal field is then passed through the medium without any loss when the two-photon resonance condition is satisfied. In this scheme, the width of the EIT window is nearly 200 kHz as shown in Fig. 4(b) (see the red curve). However, in the five-level M-type medium, the signal field is amplified due to the active Raman gain process when the pump field is present. The intensity of the signal field is increased by 3 times, and its spectrum width is about 202 kHz as shown in Fig. 4(b) (see the black curve). Due to the third-order absorption demonstrated in Eq. (5b), the intensity of the signal field decreases as the intensity of the phase-control light increases in this six-level system. In Fig. 4(a), the intensity of the signal field is plotted against the phase-control field. As the power of phase-control field increases, the signal field intensity decreases greatly due to the third-order absorption. By carefully adjusting the system parameters, we can obtain the same absorption for the EIT-type system without the phase-control field and the M-type system with the phase-control field. In Fig. 4(a), the red curve indicates the absorption for the EIT-type system, while the black curve denotes the absorption for the M-type system. The transmission rate of the signal light can be calculated by the expression $\eta_L = \exp[-2k_S \mathrm{Im}(\chi_S)L]$. Here the π nonlinear phase shift can be written into the signal field when the phase-control field is applied as demonstrated in Eq. (5). Similar to our previous works,[19,33] the nonlinear Kerr phase shift is studied by employing an optical Mach–Zehnder interferometer. The π nonlinear phase shift is observed in this hybrid scheme when the power of the phase-control field is only about 0.5 mW. Correspondingly, the intensity of the phase-control field is nearly 7 mW/cm^2.

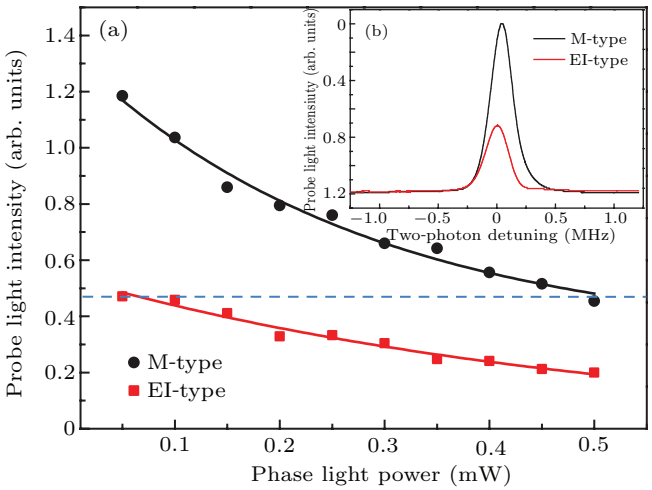


Fig. 4. (a) The intensity of the signal field plotted against the phase-control field. It is decreased, due to the third-order absorption, with increasing the power of phase-control light. (b) The intensity of the signal field plotted as a function of the two-photon detuning.

Next, we examine the frequency spectrum of the signal laser, which was measured by a microwave spectrum analyzer using the beat signal. The signal field is separated into two parts after the PBS and half-wave plate, one is signal field and the other is the reference field shown in Fig. 3. After two AOMs are used to shift the frequency of the reference field, the signal field and the reference field are combined each other using a beam splitter. In Fig. 5(a), we show the beat note signal. The red curve is the beat note spectrum between the signal field and reference field when the coupling field is present (see the EIT-type system), while the blue curve denotes the case of coexistence of the coupling field and pumping field (i.e., the M-type system). The widths of the beat note signals are 31 kHz and 53 kHz for the EIT-type and M-type schemes, respectively. The beat note spectrum is also measured when the phase-control light is present. When the power of the phase-control light is about 0.5 mW (see the black curve), its width is about 32 kHz. In Fig. 5(b), we also show the widths of the beat note signals for the different powers of the phase-control

light in the M-type scheme. Obviously, its widths is decreased greatly as the power of the phase-control field increases.

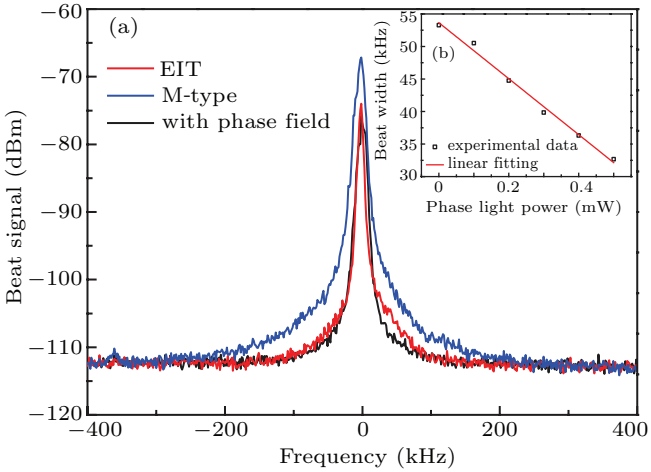


Fig. 5. (a) The beat note signals for the EIT-type system (red curve), the M-type system without the phase-control field (blue curve), and the M-type system with the phase-control field (black curve). (b) The widths of the beat note signals versus the intensity of the phase-control field. Its width is close to that of EIT when the power of the phase-control light is about 0.5 mW, where a π nonlinear phase shift is achieved.

We should point out that the intensity and frequency of the signal photons is very important in the quantum computers and communications. In Fig. 4, we can see that the intensity of the signal light is attenuated not only in the EIT-type scheme but also in the M-type scheme when the phase-control field is applied. In this phase operation, the intensity of the signal field without the phase-control light in the EIT scheme is required to be the same as its intensity with the phase-control field in the M-type scheme. At the same time, the width of the beat note signal with the phase-control field in the M-type scheme must be the same as its width without the phase-control field in the EIT-type scheme (see Fig. 5). Then, one can obtain the low noise and lossless cross phase modulation in this hybrid scheme.

In summary, we have developed a hybrid scheme for realizing strong cross phase modulation based on both electromagnetically induced transparency and active Raman gain in a multi-level atomic medium. By choosing specific system parameters, we show that the linear and the third-order absorption can be eliminated simultaneously via the Raman gain process in such a system. The cross phase modulation with low loss rate and very weak noise is demonstrated in a room-temperature ^{85}Rb vapor. We also show that the phase noise of the signal field can also be ignored when the phase control field is applied in such a hybrid scheme.

References

[1] Nielsen M A and Chuang I L 2000 *Quantum Computation and Quantum Information* (Cambridge: Cambridge University Press)
[2] Gisin N, Ribordy G W, Tittel G and Zbinden H 2002 *Rev. Mod. Phys.* **74** 145
[3] Vedral V 2007 *Introduction to Quantum Information Science* (New York: Oxford University Press)
[4] Matthews J C F 2013 *Multi-Photon Quantum Information Science and Technology in Integrated Optics* (Berlin: Springer)
[5] Lasky R C, Osterberg U L and Stigliani D P 1995 *Optoelectronics for Data Communications* 1st edn (Salt Lake City: Academic Press)
[6] Crespi A, Ramponi R, Osellame R, Sansoni L, Bongioanni I, Sciarrino F, Vallone G and Mataloni P 2011 *Nat. Commun.* **2** 566
[7] Vitali D, Fortunato M and Tombesi P 2000 *Phys. Rev. Lett.* **85** 445
[8] Ottaviani C, Vitali D, Artoni M, Cataliotti F and Tombesi P 2003 *Phys. Rev. Lett.* **90** 197902
[9] Lukin M D and Imamoglu A 2001 *Nature* **413** 273
[10] Resch K J, Lundeen J S and Steinberg A M 2002 *Phys. Rev. Lett.* **89** 037904
[11] Agrawal G P 2006 *Nonlinear Fiber Optics* 4th edn (New York: Academic Press)
[12] Schmidt H and Imamoglu A 1996 *Opt. Lett.* **21** 1936
[13] Harris S E 1997 *Phys. Today* **50** 36
[14] Kang H S and Zhu Y F 2003 *Phys. Rev. Lett.* **91** 093601
[15] Chen Y F, Wang C Y, Wang S H and Yu I A 2006 *Phys. Rev. Lett.* **96** 043603
[16] Bai J H, Li J J, Wu L A, Fu P M, Wang R Q and Zuo Z C 2017 *Chin. Phys. B* **26** 044204
[17] Wang M, Lu X G, Bai J H, Pei L Y, Miao X X, Gao Y L, Wu L A, Fu P M, Yang S P, Pang Z G, Wang R Q and Zuo Z C 2015 *Chin. Phys. B* **24** 114205
[18] Deng L and Payne M G 2007 *Phys. Rev. Lett.* **98** 253902
[19] Li R B, Deng L and Hagley E W 2013 *Phys. Rev. Lett.* **110** 113902
[20] Li R B, Deng L and Hagley E W 2014 *Phys. Rev. A* **90** 063806
[21] Hu M, Yang Y F, Zheng Y, Liu G B, Wang J H, Liu K, Chen X L, Zhao C, He B and Zhou J 2016 *Chin. Phys. Lett.* **33** 044208
[22] Cai X L, Zhou C H, Zhou D J, Liu J B, Guo J W and Gui L 2015 *Chin. Phys. Lett.* **32** 114207
[23] Lei C M, Song R, Jin A J and Hou J 2015 *Chin. Phys. Lett.* **32** 074202
[24] Zhang H N, Chen X H, Wang Q P and Li P 2015 *Chin. Phys. Lett.* **32** 014203
[25] Xu Y, Chen M, Li Z W, Bai Z X, Yang C, Chen L Y, Li G and Liu Y 2013 *Chin. Phys. Lett.* **30** 084202
[26] Shi J L, Xu J, Luo N N, Wang Q, Zhang Y B, Zhang W W and He X D 2019 *Acta Phys. Sin.* **68** 044201 (in Chinese)
[27] Sheng Z C, Wang T, Zhou G Y, Xia C M, Liu J T, Li B Y, Fan H X, Chen Y and Hou Z Y 2018 *Acta Phys. Sin.* **67** 184211 (in Chinese)
[28] Ma H M, Chen L Q and Yuan C H 2016 *Chin. Phys. B* **25** 124206
[29] Artoni M and Zavatta A 2015 *Phys. Rev. Lett.* **115** 113005
[30] Sun Y, Liu C, Chen P X and Liu L 2018 *Phys. Rev. A* **97** 023815
[31] Li R B, Zhu C J, Deng L and Hagley E W 2014 *Appl. Phys. Lett.* **105** 161103
[32] Zhu C J, Deng L and Hagley E W 2014 *Phys. Rev. A* **90** 063841
[33] Li R B, Zhu C J, Deng L and Hagley E W 2015 *Phys. Rev. A* **92** 043838